SLAC-PUB-450
(EXPI)

1.6 GeV/c CHARGED PARTICLE SPECTROMETER FACILITY AT THE STANFORD LINEAR ACCELERATOR CENTER*

by

R. Anderson, D. Gustavson, R. Prepost,† D. Ritson
Stanford Linear Accelerator Center
Stanford, California

ABSTRACT

A 1.6 GeV/c spectrometer has been constructed at SLAC incorporating an $n = 0$, 90° bend, 254cm radius magnet with second-order corrections. The magnet is of the window frame type allowing invariant focal properties up to 21kg. It has a momentum resolution of $\pm$ 0.08% and an angular resolution of $\pm$ 0.4mrad. It simultaneously focusses production angle and momentum from a 20cm long target onto a single focal plane orthogonal to the beam direction allowing a considerable simplification in detecting a high energy scattering process.

(To be printed in Nuclear Instr. and Methods)

---

*Work supported by the U. S. Atomic Energy Commission.

† Now at Department of Physics, University of Wisconsin, Madison, Wisconsin

1.6 GeV/c CHARGED PARTICLE SPECTROMETER FACILITY
AT THE STANFORD LINEAR ACCELERATOR CENTER

INTRODUCTION

The SLAC 1.6 GeV/c spectrometer is mounted on a common pivot with two other SLAC spectrometers, the 8 and 20 GeV/c spectrometers. It is a weak focussing ($n = 0$) 90° vertical bend device with a maximum acceptance exceeding 3-millisteradians of solid angle, 20cm of target length and $\pm$ 5% in momentum. Angled entrance and exit faces introduce first-order focussing conditions which make the production angle and momentum focal planes coincident in space. This feature simplifies the detector arrays required for the analysis of high energy physics experiments.

The production angle versus momentum display in the focal plane has a linear dispersion of 4.19cm per percent in momentum and 0.808cm per milliradian in angle, with a resolution of $\pm$ 0.08% in momentum and $\pm$ 0.4 milliradian in angle. This degree of resolution is required to kinematically separate processes differing by the production of only one π-meson. This display is convenient since the kinematics of 2-body processes give an approximately linear relation between production angle and momentum over the small region seen by the spectrometer at any one setting. The focus of particles from a particular two body process is approximately a straight line in the focal plane, and can be selectively detected by appropriate scintillation counters. In practice, the focal plane is divided into strips by the hodoscope counters which can be rotated into alignment along the appropriate kinematic curve. This technique thus eliminates the complex decoding necessary for systems which use separate hodoscopes for both angle and momentum measurements, and makes it possible to count particles at 100 megacycle rates with relatively simple electronic systems. To maintain good resolution for this mode of operation, the first-order corrections were adjusted to make the momentum and production angle planes coincide, and second-order corrections were made so that the focal planes were normal to the central ray.

The use of a homogeneous n = 0 magnetic field [1] made it possible to utilize a window frame design and thus to operate the magnet without any appreciable saturation or change in focussing properties up to fields of 21 kilogauss.

The second-order corrections were introduced by shaping the pole faces slightly in three "beta lens" regions to produce $\beta \neq 0$ but leaving $n = 0$. [2] The boundaries of the correction region and the entrance and exit regions were shaped to minimize saturation effects. The appropriate values of the design parameters were found with the aid of the results of K. Brown [3] for the second-order transfer matrix of a homogeneous field magnet and the SLAC TRANSPORT program.[4] The measured magnet properties were within the design specifications without need for any shimming of the field.

---

(1) J. V. Allaby and D. M. Ritson, Rev. Sci. Instr. 36, No. 5, 607(May, 1965)

(2) $n = -\frac{r_o}{B_o}\frac{\partial B}{\partial r}$ and $\beta = \frac{1}{2}\left(\frac{r_o^2}{B_o}\frac{\partial^2 B}{\partial r^2}\right)$ notation of SLAC-75 by K. L. Brown

(3) c.f., K. Brown, SLAC Report No. 75, 1967 and K. Brown, "Advances in High Energy Physics", Cool and Marshak, Vol.1 in press for reviews of relevant formalae and methods.

(4) SLAC-DOC-12, TRANSPORT by S. Howry, C. H. Moore, S. H. Butler, October, 1963.

THEORY AND DESIGN PARAMETERS

The choice of design characteristics was made in the following way. Edge focussing was introduced at the entrance face of the magnet to obtain parallel-to-point focussing in the non-bend plane. However, the introduction of such focussing in the non-bend plane decreases the focussing in the bend plane and results in a momentum focal plane at an inconvenient distance from the magnet. By introducing compensating focussing at the exit to the magnet it is possible to make the focal planes in both the horizontal and vertical dimensions coincide at 254cm from the exit to the magnet. Fig. 1 shows diagrammatically the first-order focussing properties of the magnet in the horizontal and vertical dimensions.

Second-order corrections were made in order to minimize the "circle of confusion" in a focal plane orientated at right angles to the direction of the incident particles. The numerical derivatives of the various aberrations with respect to the strengths of the second-order correcting elements were obtained from the SLAC TRANSPORT program and fed into the set of minimal equations which were then solved for the appropriate corrections. This procedure led to the values chosen for our design. Had the only criterion been to minimize the "circle of confusion", one second-order correction on the front face of the magnet would have been the optimum design choice. Since two second-order correction regions did not allow us to simultaneously achieve a reasonably small circle of confusion and a focal plane orthogonal to the beam direction, three second-order correction regions were required. These three correction regions are referred to as "β-lenses" since in the lens region β is non-zero.[2] The β-lenses are shown in Figs. 2a and 2b.

CONSTRUCTION

Fig. 3 shows a view of the complete spectrometer including the magnet, carriage, and shielding. The magnet is mounted on a carriage which is pivoted on the target support and rolled on a 7.6m diameter circular rail so the particle trajectories are bent upwards. An angle readout driven by a chain mounted on the rail makes it possible to have a remote digital readout of the laboratory angle to .001 degrees. The magnetic field of the spectrometer is measured using an NMR probe that swings into the center of the magnetic gap where the uniform magnetic field gives very clean NMR signals. The space traversed by the particles from target to counters is enclosed by a vacuum chamber. An aperture stop made of four moveable tungsten lined jaws makes it possible to define both the vertical and horizontal acceptance angles. The horizontal aperture stop is especially useful since it allows the target length to be clearly defined. The spectrometer angle, magnet current, aperture stop and NMR probe are all remotely controlled. The carriage also supports a cylindrical concrete and steel shielding house which protects the detectors from room background. Two moveable lead doors 2-ft. thick, each weighing 14-tons, allow access to the detector cave. The concrete shielding is made in circular segments to simplify construction and assembly. Their size was dictated by the 50-ton capability of the crane servicing the spectrometer. The counter assembly may be rotated remotely in order to align the hodoscope counters along the desired direction in the focal plane. The counters are also accessible by removing the top concrete shielding block. This is the primary access route for installing and removing the large counter assemblies. The access afforded by the doors is used for minor repairs and adjustments.

PERFORMANCE

Before the spectrometer was mounted together with its shielding, its properties were checked with floating wire techniques as described by Allaby and Ritson.(1) Fig. 4 shows the results of some of these measurements. No difference in the properties of the spectrometer from those predicted by theory were detected by the wire floats except for extreme rays that passed close to the magnet coils. After completion of the wire float measurements, the electron beam of the SLAC accelerator was used to further explore the properties of the spectrometer; particularly those of the non-bend plane. A test system designed for the S.L.A.C. 8 and 20 GeV/c spectrometers was used to steer the beam, and zinc sulfide screens at the entrance and focal plane of the spectrometer were used to observe the properties of the magnet for different entrance angles and displacements.

The positions of the momentum and angle focal planes were checked to within a few inches with the wire float and beam surveys. In general, second-order coefficients were too small to be measured. Rays outside the central two-thirds of the aperture showed a drastic deterioration of the focussing properties, presumably due to fringe fields. The origins of this effect have not been further investigated, but could presumably be considerably reduced if desired, by further shaping of the magnet pole tips. The magnetic field had an effective net 4.1cm additional length above that expected from the design. Fig. 5 shows a typical magnet excitation curve. The magnet begins to slightly saturate at central fields of 18 kilogauss, but showed no appreciable change in focussing properties up to central fields of 21 kilogauss.

Table I lists the properties of the spectrometer. Table II compares the measured and theoretical values of the focussing properties. Agreement is well within the measurement errors. As the first-order properties should be determined well by the geometry of the system, we believe that the predicted first-order values are close to being correct. If the first-order momentum dispersion, and the first-order angular dispersion are known for displacements about the central ray, the acceptance of the instrument when used with a symmetrically placed counter system is determined up to second-order (second-order corrections when averaged over a symmetric detector assembly average to zero). Accordingly, we believe that this instrument can be trusted to an accuracy of the order of 3% when used to make absolute measurements with a symmetric detector.

SUMMARY

We have constructed a charged particle spectrometer for use with the S.L.A.C. 20 GeV/c electron accelerator for measuring and detecting charged particles with momenta up to 1.6 GeV/c. The instrument is precise, flexible, and particularly adapted to measurements with a high energy accelerator.

ACKNOWLEDGEMENTS

We would like to thank Karl Brown for indispensable help with the design parameters of the magnet, and with the problems associated with second-order corrections.

We are indebted to Jobst Brandt who supervised the mechanical design and the construction of the spectrometer and to Bob Eisele who made the many drawings. We would like to thank Bill Davies-White for the construction of the angular readout of the spectrometer and for his help in surveying the spectrometer into position. We would like to express our appreciation to Ed Taylor and his engineering staff for the general support in the construction and servicing of the spectrometer without which the spectrometer facility could not have been put into operation in such a short time. We would like to thank Dr. G. Jones and D. Kreinick for their assistance in the wire float measurements. Finally, we would like to thank John Grant for his invaluable help in making mechanical devices and attachments for the spectrometer.

TABLE I

Spectrometer Parameters

Maximum momentum	1.60 GeV/c
Maximum field	21.0 kg
Maximum current	2840 amperes
Voltage at 21.0 kg	440 volts
Maximum power	1.25 MW
Momentum dispersion	4.19cm per % momentum
Momentum resolution	± 0.08%
Momentum acceptance	± 5%
Horizontal angular acceptance*	± 17 mrad
Vertical angular acceptance	± 60 mrad
Solid angle	4.1 millisteradian
Angular dispersion	.823 cm/mr
Angular resolution $\Delta\theta$	± .37
Target length	20cm
Radius of central ray	254cm
Focal lengths	254cm
Field index	n = 0, 90° arc
Entrance β **	11.5
Central β	-10.0
Exit β	10.0
Entrance face angle	28°
Exit face angle	22°
Number of turns	144
Average length of each turn	9.1m
Number of turns/water circuit	3
Conductor size	1.59 × 1.80cm
Diameter of hole in conductors	.95cm
Conductor area	2.13cm^2
Weight of magnet iron	78 tons
Weight of copper conductor	1.8 tons
Weight of shielding	205 tons
Weight of carriage	15 tons

*Bend plane is vertical

**The three β sections each are 50.8cm in length.

TABLE II

Measured and theoretical values of some of the 1st and 2nd order coefficients of the magnet.

COEFFICIENT	THEORETICAL VALUE	EXP. VALUE	SOURCE OF MEASUREMENT
$\langle x\|\delta\rangle$ the momentum dispersion	4.19cm per %	$4.19 \pm .05$cm/%	Wire float
$\langle y\|\phi_o\rangle$ the angular dispersion	0.823cm per mr	$0.808 \pm .038$cm per mr	Electron Beam spot survey
$\langle \theta\|\theta_o\rangle$ A relation of input to output angles	1.514	$1.52 \pm .02$	Wire float
$\langle x\|\delta^2\rangle$	6.07×10^{-2} cm/(%)^2	$4.95 \pm 1.0\times10^{-2}$cm per % squared	Wire float
$\langle y\|\phi_o\delta\rangle$	1.25×10^{-2} cm/mr %	1.24×10^{-2} per % per mr	Electron Beam Spot Survey
$\langle x\|\theta_o\delta\rangle$	1.03×10^{-3} cm/mr %	≈ 0	Electron Beam Spot Survey
$\langle x\|\theta_o^2\rangle$	2.47×10^{-4} cm/(mr)^2	$\approx 2.5 \times 10^{-4}$	Electron Beam Spot Survey

The notation used is that given by K. Brown.(3)

δ is the momentum difference from the central orbit.

x is the displacement at the focal plane along the "momentum" axis.

θ_o is the input angle in the momentum plane.

θ is the output angle in the momentum plane.

y is the displacement along the "angular axis" in the focal plane.

ϕ_o is the input "production" angle.

APPENDIX A

This appendix contains the first-order and second-order printouts of the TRANSPORT Computer Program.

Table III shows the first-order coefficients of a Taylor series expansion for the coefficients x, θ, y, φ, z, and δ. These variables and the convention used for the curvilinear coordinate system of TRANSPORT are defined in SLAC-75 by Karl L. Brown. The reader is referred to this report for a complete definition of all symbols.

Table IV shows the complete second-order set of the Taylor series coefficients. The variables are labeled 1, 2, 3, 4, 5, 6 which correspond to x, θ, y, φ, z, and δ. Thus, for example, the coefficient labeled 1 22 is the Taylor series coefficient $\langle x|\theta_o^2\rangle$. Units for the variables in Tables III and IV are cm for x, y, and z; milliradians for θ and φ; and per cent for δ.

TABLE III

First-Order Transform

	x_o	θ_o	y_o	φ_o	z_o	δ_o
x	-0.661	0.0	0.0	0.0	0.0	4.190
θ	-4.610	-1.514	0.0	0.0	0.0	6.427
y	0.0	0.0	0.0	0.823	0.0	0.0
φ	0.0	0.0	-1.220	1.356	0.0	0.0
z	-1.508	-0.635	0.0	0.0	1.000	-1.460
δ	0.0	0.0	0.0	0.0	0.0	1.000

TABLE IV

*2nd ORDER TRANSFORM

1 11	- 0.641E-03										
1 12	1.411E-04	1 22	- 2.465E-04								
1 13	0.0	1 23	0.0	1 33	0.704E-03						
1 14	0.0	1 24	0.0	1 34	4.227E-04	1 44	3.554E-04				
1 15	0.0	1 25	0.0	1 35	0.0	1 45	0.0	1 55	0.0		
1 16	1.141E-02	1 26	- 1.027E-03	1 36	0.0	1 46	0.0	1 56	0.0	1 66	- 6.066E-02
2 11	0.180E-01										
2 12	0.413E-02	2 22	- 1.945E-03								
2 13	0.0	2 23	0.0	2 33	- 0.227E-01						
2 14	0.0	2 24	0.0	2 34	- 0.681E-02	2 44	3.207E-03				
2 15	0.0	2 25	0.0	2 35	0.0	2 45	0.0	2 55	0.0		
2 16	- 2.129E-02	2 26	- 3.508E-02	2 36	0.0	2 46	0.0	2 56	0.0	2 66	- 1.927E-01
3 11	0.0										
3 12	0.0	3 22	0.0								
3 13	2.993E-02	3 23	1.801E-03	3 33	0.0						
3 14	5.302E-03	3 24	5.492E-04	3 34	0.0	3 44	0.0				
3 15	0.0	3 25	0.0	3 35	0.0	3 45	0.0	3 55	0.0		
3 16	0.0	3 26	0.0	3 36	2.034E-02	3 46	1.253E-02	3 56	0.0	3 66	0.0
4 11	0.0										
4 12	0.0	4 22	0.0								
4 13	0.577E-01	4 23	3.791E-03	4 33	0.0						
4 14	0.792E-02	4 24	2.241E-03	4 34	0.0	4 44	0.0				
4 15	0.0	4 25	0.0	4 35	0.0	4 45	0.0	4 55	0.0		
4 16	0.0	4 26	0.0	4 36	0.517E-01	4 46	5.557E-02	4 56	0.0	4 66	0.0
5 11	0.296E-02										
5 12	- 1.790E-04	5 22	- 5.800E-04								
5 13	0.0	5 23	0.0	5 33	- 1.030E-02						
5 14	0.0	5 24	0.0	5 34	- 3.760E-03	5 44	- 8.544E-04				
5 15	0.0	5 25	0.0	5 35	0.0	5 45	0.0	5 55	0.0		
5 16	0.411E-02	5 26	- 8,967E-04	5 36	0.0	5 46	0.0	5 56	0.0	5 66	- 2.393E-03
6 11	0.0										
6 12	0.0	6 22	0.0								
6 13	0.0	6 23	0.0	6 33	0.0						
6 14	0.0	6 24	0.0	6 34	0.0	6 44	0.0				
6 15	0.0	6 25	0.0	6 35	0.0	6 45	0.0	6 55	0.0		
6 16	0.0	6 26	0.0	6 36	0.0	6 46	0.0	6 56	0.0	6 66	0.0

FIGURE CAPTIONS

Fig. 1 First-order focal properties.

Fig. 2 (2a) Shows the magnet and coils. The angled entrance and exit faces cause the angle and momentum focal planes to coincide. The three beta lenses give second-order corrections and rotate the focal plane so it is perpendicular to the central ray.

(2b) Shows a cross-sectional view of the beta lenses.

Fig. 3 The complete spectrometer.

Fig. 4 Wire float trajectories near the focal plane, for five momenta and a range of entrance angles. In normal use the dashed rays are blocked by an entrance mask. The percentage change in momentum from the central ray is δ. The number by each ray is the angle in milliradians between it and the central rays before entering the spectrometer. All rays pass through the target point.

Fig. 5 Excitation curve of the spectrometer. 1.60 GeV/c corresponds to 21.0 kg.

(a)

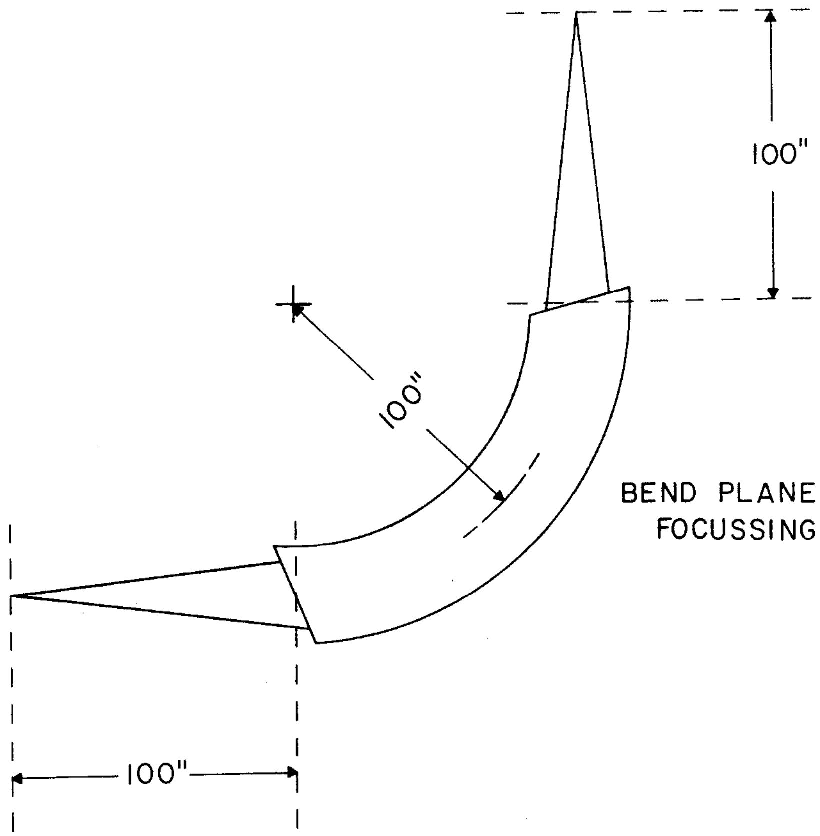
100"
100"
BEND PLANE
FOCUSSING
100"

(b)

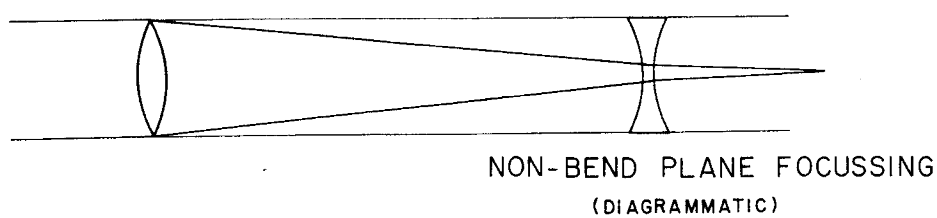
NON-BEND PLANE FOCUSSING
(DIAGRAMMATIC)

Fig. 1

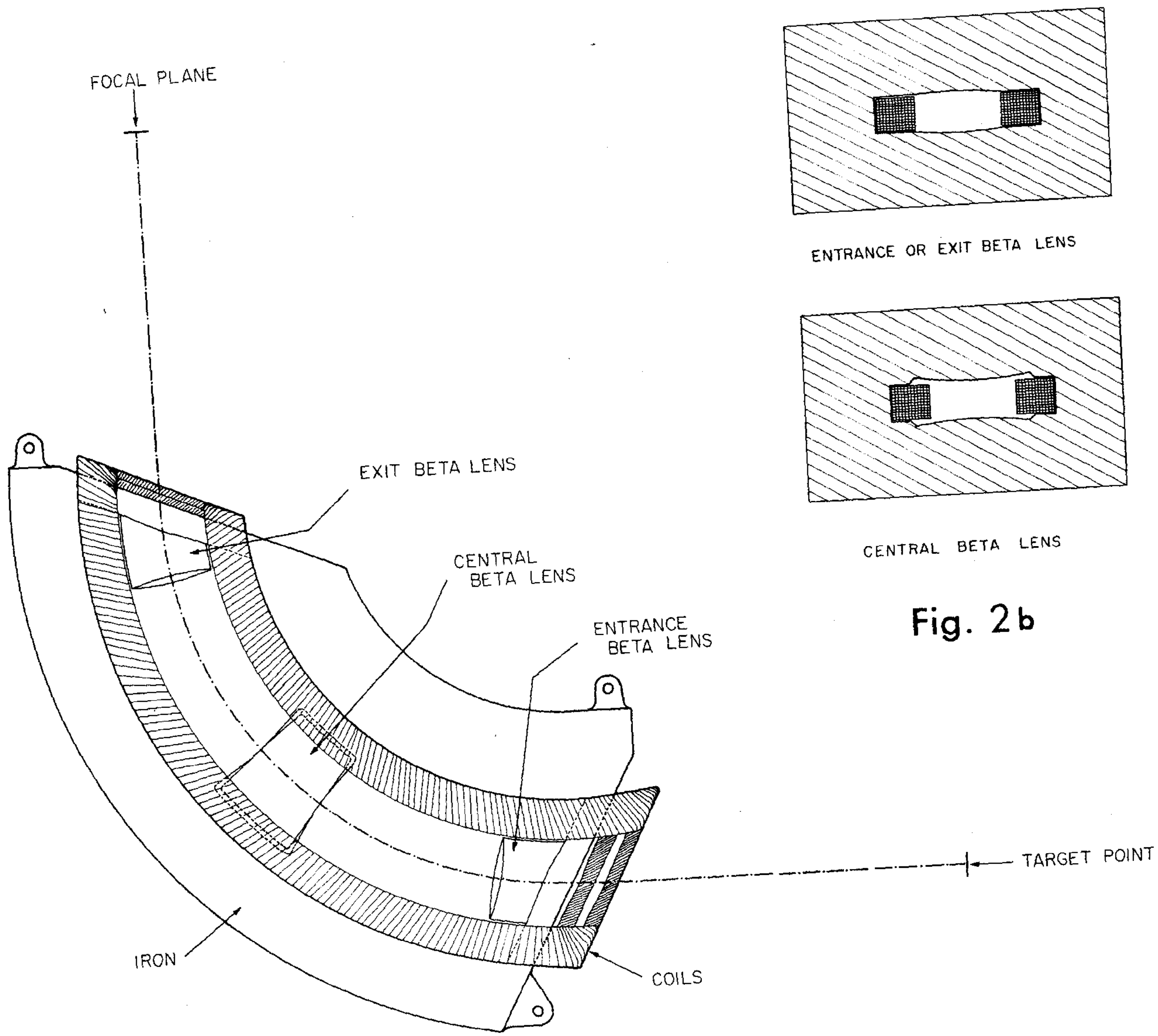

FOCAL PLANE
EXIT BETA LENS
CENTRAL
BETA LENS
ENTRANCE
BETA LENS
TARGET POINT
IRON
COILS
ENTRANCE OR EXIT BETA LENS
CENTRAL BETA LENS

Fig. 2b

Fig. 2a

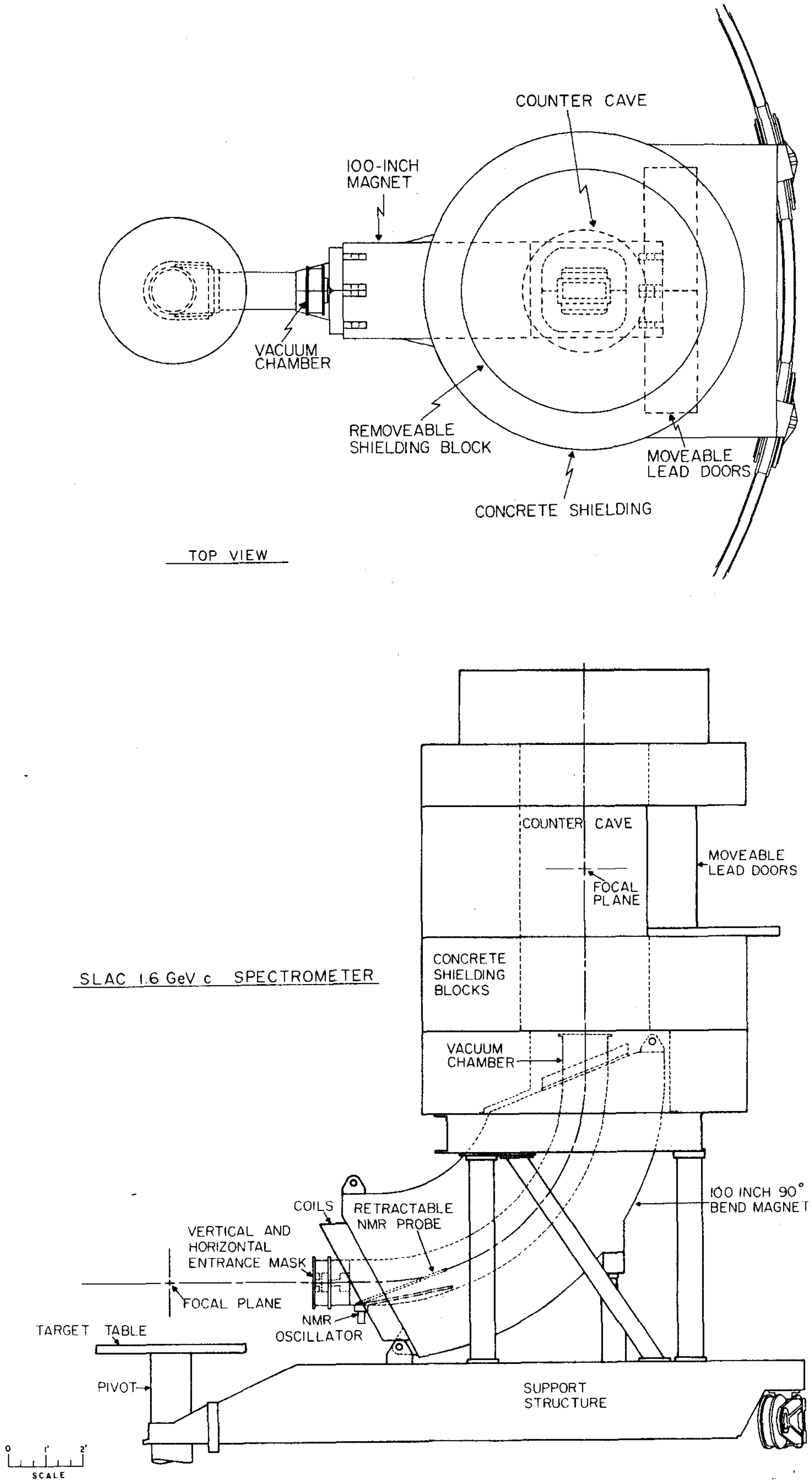
COUNTER CAVE
100-INCH MAGNET
VACUUM CHAMBER
REMOVEABLE SHIELDING BLOCK
MOVEABLE LEAD DOORS
CONCRETE SHIELDING
TOP VIEW
COUNTER CAVE
MOVEABLE LEAD DOORS
FOCAL PLANE
SLAC 1.6 GeV c SPECTROMETER
CONCRETE SHIELDING BLOCKS
VACUUM CHAMBER
100 INCH 90° BEND MAGNET
COILS
RETRACTABLE NMR PROBE
VERTICAL AND HORIZONTAL ENTRANCE MASK
FOCAL PLANE
NMR OSCILLATOR
TARGET TABLE
PIVOT
SUPPORT STRUCTURE
0 1' 2'
SCALE

Fig. 3

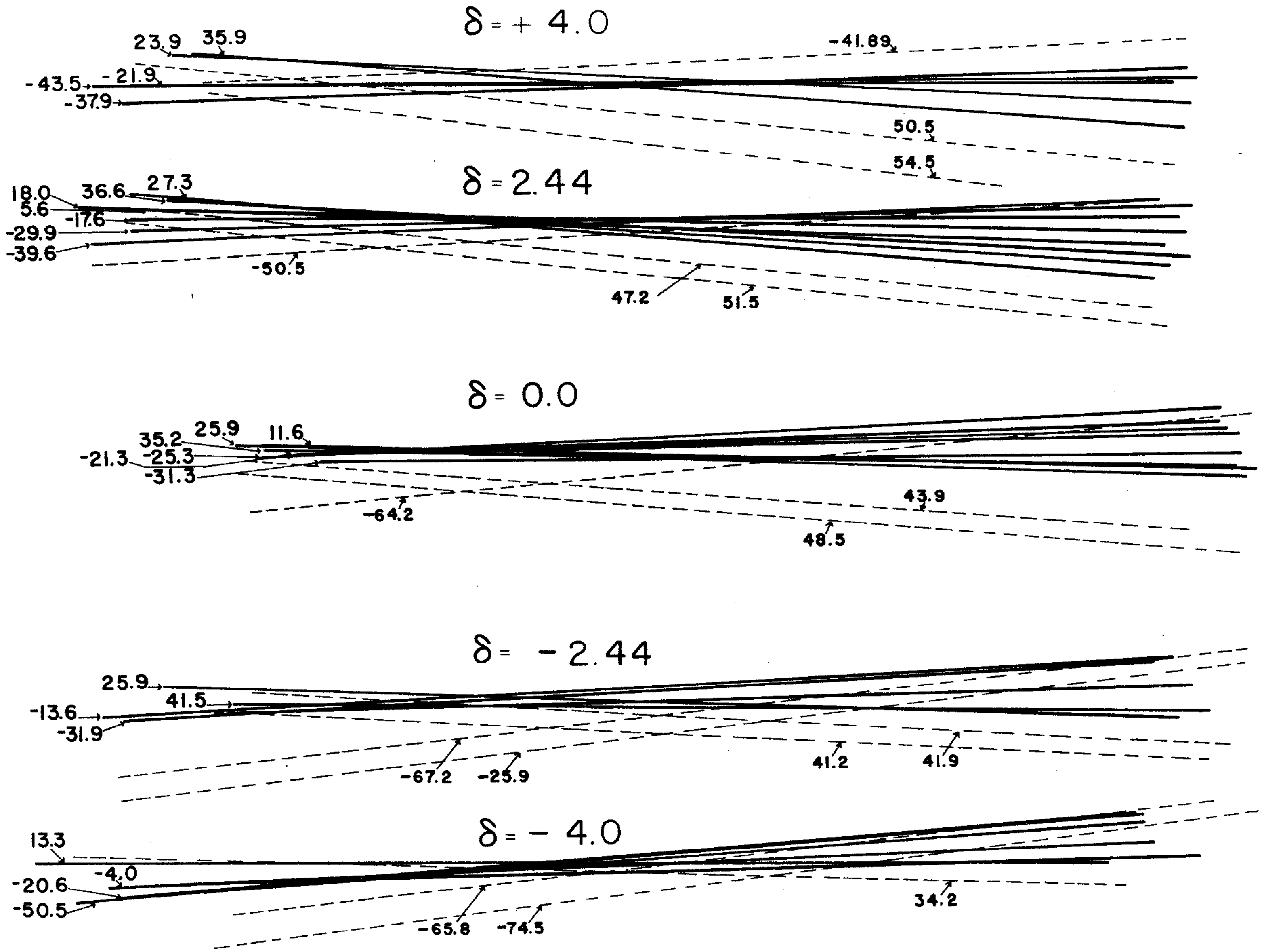

δ = + 4.0
23.9
35.9
-41.89
-43.5
- 21.9
-37.9
50.5
54.5
δ = 2.44
18.0
36.6
27.3
5.6
-17.6
-29.9
-39.6
-50.5
47.2
51.5
δ = 0.0
35.2
25.9
11.6
-21.3
-25.3
-31.3
-64.2
43.9
48.5
δ = -2.44
25.9
41.5
-13.6
-31.9
-67.2
-25.9
41.2
41.9
δ = - 4.0
13.3
-4.0
-20.6
-50.5
-65.8
-74.5
34.2

Fig. 4

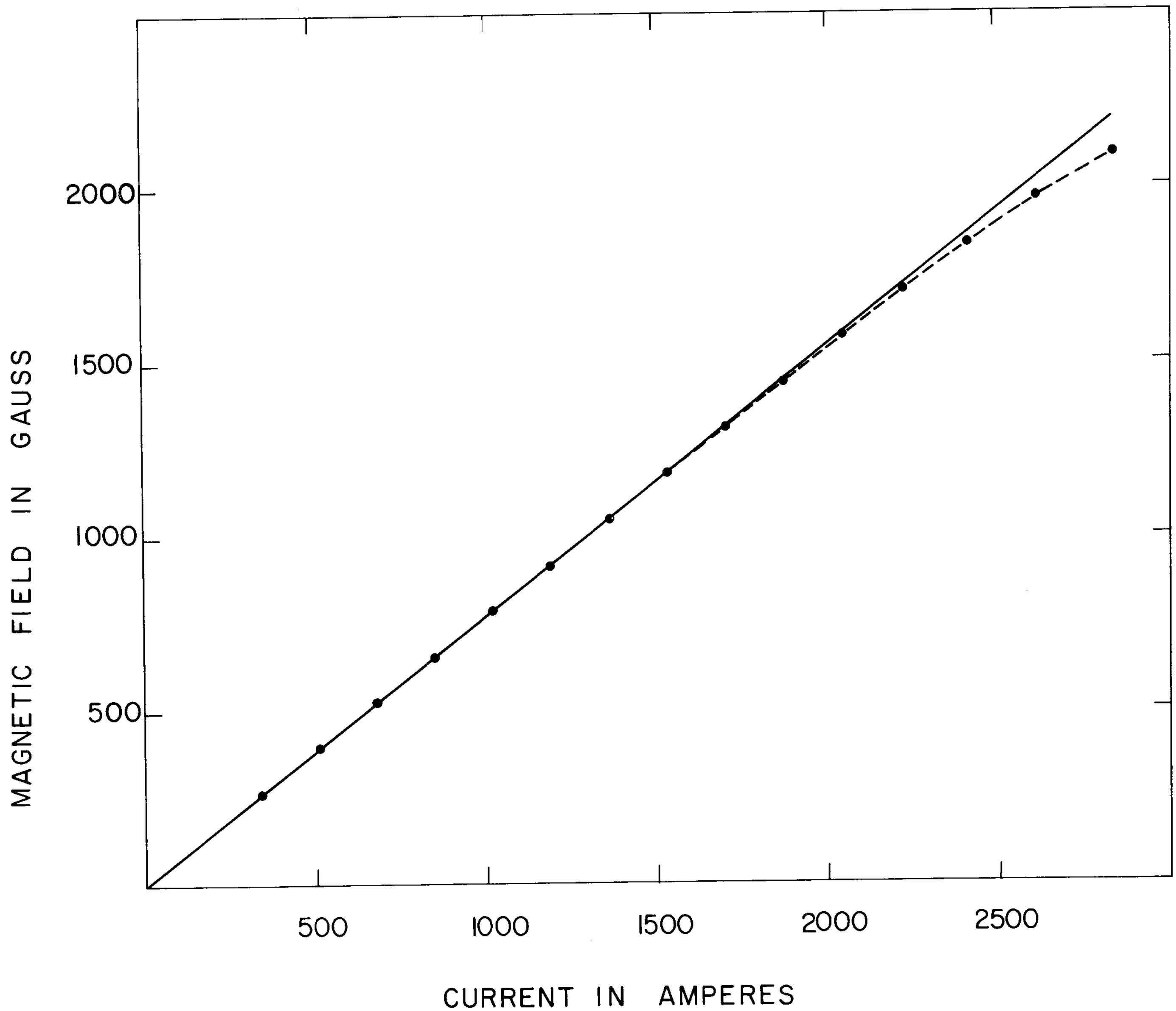

2000
1500
1000
500
MAGNETIC FIELD IN GAUSS
500
1000
1500
2000
2500
CURRENT IN AMPERES

Fig. 5